

UIP2P: Unsupervised Instruction-based Image Editing via Edit Reversibility Constraint

Enis Simsar¹ Alessio Tonioni³ Yongqin Xian³ Thomas Hofmann¹ Federico Tombari^{2,3}
¹ETH Zürich - DALAB ²Technical University of Munich ³Google Switzerland
<https://uip2p.github.io>

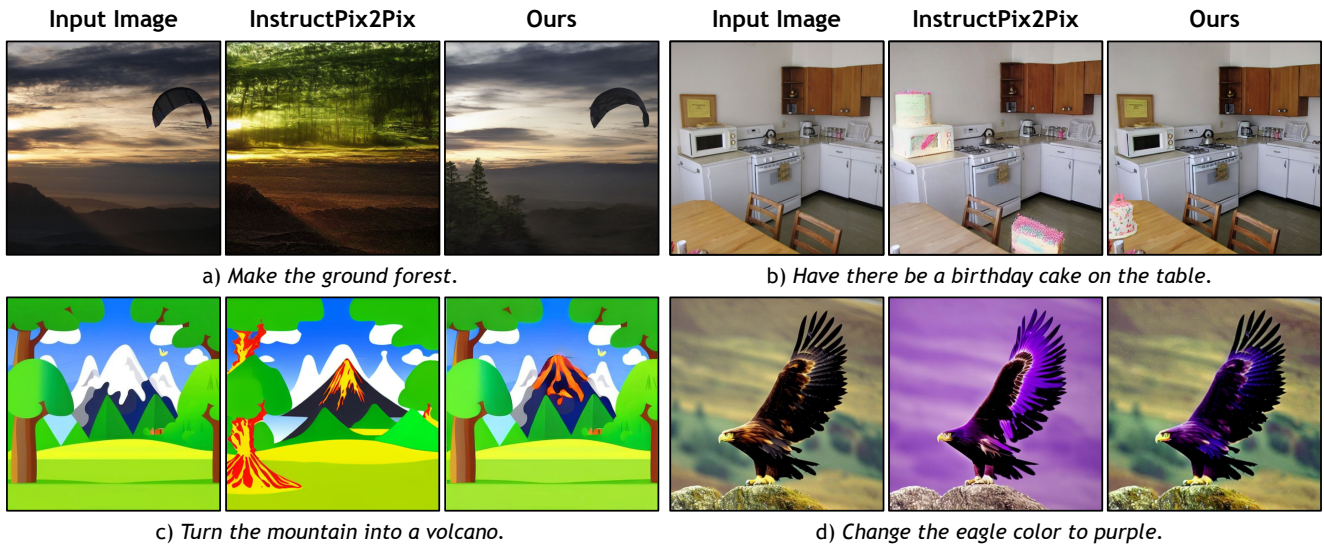


Figure 1. **Unsupervised InstructPix2Pix**. Our approach applies more precise and coherent edits while better preserving scene structure. UIP2P surpasses the supervised alternative, IP2P, trained on a synthetic dataset, demonstrating superior performance on both real (a, b) and synthetic (c, d) images.

Abstract

We propose an unsupervised instruction-based image editing approach that removes the need for ground-truth edited images during training. Existing methods rely on supervised learning with triplets of input images, ground-truth edited images, and edit instructions. These triplets are typically generated either by existing editing methods—introducing biases—or through human annotations, which are costly and limit generalization. Our approach addresses these challenges by introducing a novel editing mechanism called *Edit Reversibility Constraint (ERC)*, which applies forward and reverse edits in one training step and enforces alignment in image, text, and attention spaces. This allows us to bypass the need for ground-truth edited images and unlock training for the first time on datasets comprising either real image-caption pairs or image-caption-instruction triplets. We empirically show that our approach performs better across a broader range

of edits with high-fidelity and precision. By eliminating the need for pre-existing datasets of triplets, reducing biases associated with current methods, and proposing ERC, our work represents a significant advancement in unblocking scaling of instruction-based image editing.

1. Introduction

Diffusion models (DMs) have recently made significant advancements in generating high-quality and diverse images, driven largely by breakthroughs in text-to-image generation [19, 38, 39, 41]. This progress has enabled various techniques for tasks such as personalized image generation [13, 40, 53], context-aware inpainting [29, 32, 57], and image editing based on textual prompts [2, 9, 17, 23, 30]. Beyond prompt-based editing, DMs have demonstrated strong capabilities in instruction-based editing, where edits are guided by explicit natural language commands, such as instructions [6, 12, 20, 21, 58, 59].

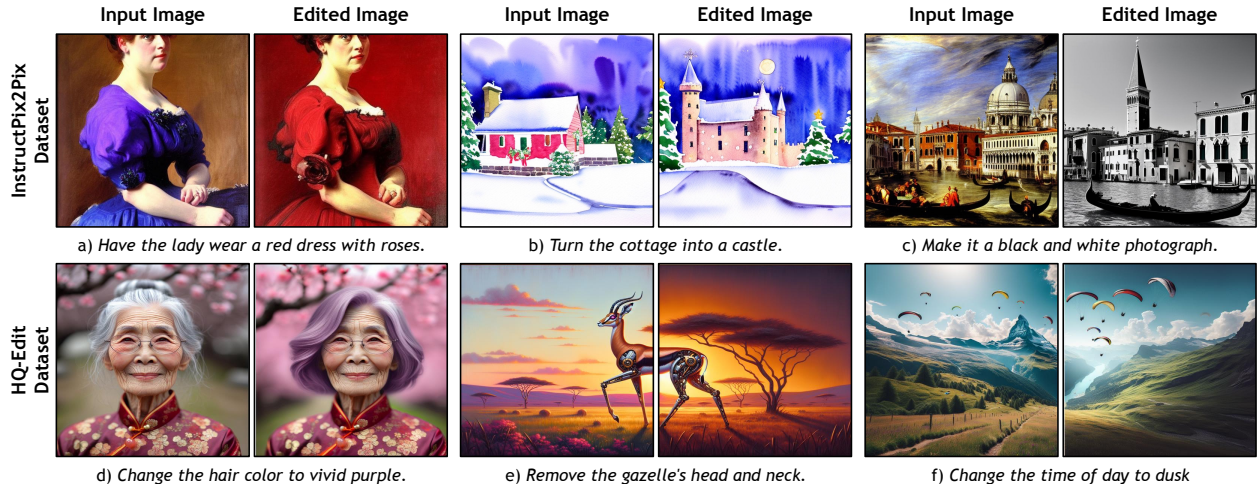


Figure 2. **Supervision Biases in InstructPix2Pix and HQ-Edit datasets.** Each example shows an input image and its corresponding ground-truth edited image for the given edit instruction. InstructPix2Pix employs Prompt-to-Prompt, while HQ-Edit uses DALL-E 3 and GPT-4V. (a & d) *Attribute-entangled edits*: Modifying a specific feature, such as clothing or hair color, unintentionally alters surrounding textures or elements. (b & e) *Scene-entangled edits*: Transforming objects, like turning a cottage into a castle or removing an element, affects unintended parts of the scene. (c & f) *Global changes*: Edits like converting an image to black and white or changing the time of day introduce widespread scene modifications, often compromising visual preservation.

However, existing methods predominantly rely on supervised learning with ground-truth edited images, *i.e.*, requiring datasets of triplets containing input images, edited images, and edit instructions [6, 12, 21, 58, 59]. These datasets are often generated using existing editing methods, such as Prompt-to-Prompt [17], or more recently, advanced diffusion and multimodal models like DALL-E 3 [4] and GPT-4V [1], as in the HQ-Edit dataset [21]. While automated approaches enable scalable dataset creation, they introduce biases (see Fig. 2), including (a & d) attribute-entangled edits that unintentionally alter surrounding elements, (b & e) scene-entangled edits, and (c & f) global changes that significantly modify the entire scene. Conversely, while valuable, human-annotated data [58] is impractical for large-scale training due to the high cost and effort involved. Reliance on automated or human-generated ground-truth edits limits the diversity of achievable modifications, constraining the development of models capable of accurately understanding and executing user instructions.

We present UIP2P, an unsupervised training for instruction-based image editing that eliminates the reliance on triplet datasets, whether generated or human-annotated, by introducing the Edit Reversibility Constraint (ERC)—a constraint enforced while training through forward and reverse edits. Instead of relying on explicitly supervised edited images, we ensure that modifications remain precise and follow the given instructions by leveraging CLIP’s ability to align text and images in a shared embedding space [37]. Additionally, we explicitly enforce alignment between forward and reverse edits in both the image and

attention spaces, enabling UIP2P to accurately interpret and localize user instructions while ensuring edits remain coherent and reflect the intended changes. ERC allows UIP2P to preserve the integrity of the original content while making precise adjustments, further enhancing the reliability of the edits. Some previous methods have enforced cycle consistency within predefined domain transformations [25, 47, 54, 56, 62]. In contrast, our constraint applies to any arbitrary pair of forward and reverse edits within a single training step, leveraging the expressive power of modern diffusion models to ensure flexibility across diverse editing tasks. By eliminating the dependence on pre-existing datasets, our approach enables training on large-scale real-image datasets—a capability previously constrained by the limitations of existing methods and the high cost of human labeling. As a result, UIP2P significantly expands the scope and scalability of instruction-based image editing compared to prior approaches. Our key contributions are as follows:

- We propose UIP2P, an unsupervised training approach for instruction-based image editing that eliminates the need for ground-truth edited images. By doing so, UIP2P offers a more scalable solution while reducing the biases inherent in alternative supervised methods.
- We introduce the Edit Reversibility Constraint (ERC), a novel mechanism that ensures edits remain stable when applying both forward and reverse edits, preserving structural integrity in the image, text and attention space. This enables precise, high-fidelity modifications that accurately reflect user instructions.

- Our approach demonstrates scalability and versatility across various real-image datasets, allowing a broad range of edits without relying on pre-existing datasets, significantly expanding the capabilities of instruction-based image editing.

2. Related Work

CLIP-Based Image Manipulation. StyleCLIP [34] combines StyleGAN and CLIP for text-driven image manipulation, requiring optimization for each specific edit. Similarly, StyleGAN-NADA [14] enables zero-shot domain adaptation by using CLIP guidance to modify generative models. While these approaches allow for flexible edits, they often rely on domain-specific models or optimization processes for each new task. These works illustrate the potential of CLIP’s powerful semantic alignment for image manipulation, which motivates the use of CLIP in other generative frameworks, such as diffusion models.

Text-based Image Editing with Diffusion Models. One common approach in image editing is to use pre-trained diffusion models by first inverting the input image into the latent space and then applying edits through text prompts [9, 17, 22, 30, 31, 33, 51, 52, 55]. For example, DirectInversion [22] edits the image after inversion using Prompt-to-Prompt [17], but the inversion step can lead to losing essential details from the original image. Additionally, methods like DiffusionCLIP [25], CycleDiffusion [54], CycleNet [56], and DualDiffusion [47] explore *domain-to-domain translation* as a way to propose image editing, by using textual prompt or without any conditions. However, their focus on translating between two fixed domains makes it difficult to handle complex edits, such as the insertion or deletion of objects. In contrast, our approach is designed for general-purpose instruction-based image editing without being restricted to domain translation, enabling greater flexibility in handling a broader range of modifications.

Instruction-based Image Editing with Diffusion Models. Another line of methods for image editing involves training models on datasets containing triplets of input image, edit instruction, and edited image [6, 21, 58, 59]. These methods, since they directly take the input image as a condition, do not require an inversion step. InstructDiffusion [15] builds on InstructPix2Pix by handling a wider range of vision tasks but has difficulty with more advanced reasoning. MGIE [12] improves on this by using large multimodal language models to generate more precise instructions. SmartEdit [20] goes a step further by introducing a Bidirectional Interaction Module that better connects the image and text features, improving its performance in challenging editing scenarios. UltraEdit [60] scales instruction-based editing to larger datasets and models, demonstrating improved performance on fine-grained editing tasks.

A major challenge in instruction-based image editing is the need for large-scale, high-quality triplet datasets. InstructPix2Pix [6] partially addresses this by generating extensive datasets using GPT-3 [7] and Prompt-to-Prompt [17]. However, while this mitigates data scarcity, it introduces issues like model biases from Prompt-to-Prompt. MagicBrush [58] tackles the quality aspect with human-annotated datasets, but this approach is small-scale, limiting its practicality for broader use.

Our method leverages CLIP’s semantic space for aligning images and text, providing a more robust solution. Moreover, Edit Reversibility Constraint (ERC) tackles both dataset limitations and biases by enforcing coherence between forward and reverse edits. Our approach enhances scalability and precision for complex instructions and eliminates the dependency on triplet datasets, making it applicable to any image-caption dataset of real images. Moreover, as ERC modifies only the training objectives of InstructPix2Pix, it integrates seamlessly with any model extension.

3. Background

Our method builds upon InstructPix2Pix (IP2P) [6], which uses Stable Diffusion’s U-Net architecture [39] for instruction-based image editing. IP2P conditions the model on both input images and text instructions using classifier-free guidance [18]. Cross-attention mechanisms compute attention maps based on text conditioning, enabling localized edits by focusing on relevant image regions.

IP2P trains on triplets of input images, edit instructions, and edited images generated using Prompt-to-Prompt [17]. However, this reliance on synthetic data introduces limitations: (1) poor generalization to real-world images, and (2) inherited biases from Prompt-to-Prompt, as shown in Fig. 2.

4. Method

We introduce UIP2P, an unsupervised diffusion-based framework for instruction-based image editing, enforcing the Edit Reversibility Constraint (ERC) to ensure that applied edits can be undone using corresponding reverse instructions. Unlike prior methods reliant on synthetic triplets or domain-specific transformations, UIP2P operates on real-world image-captions datasets without needing edit pairs. Our approach integrates text-image alignment, attention-based localization, reconstruction fidelity, and efficient noise prediction, enabling precise and generalizable edits. Additionally, we leverage LLM-generated reverse instructions, eliminating the need for requiring supervision while significantly improving scalability. In the following sections, we describe our approach in detail, including the key components of our framework (Sec. 4.1), the loss functions that enforce edit reversibility, and the training data generation procedure (Sec. 4.2).

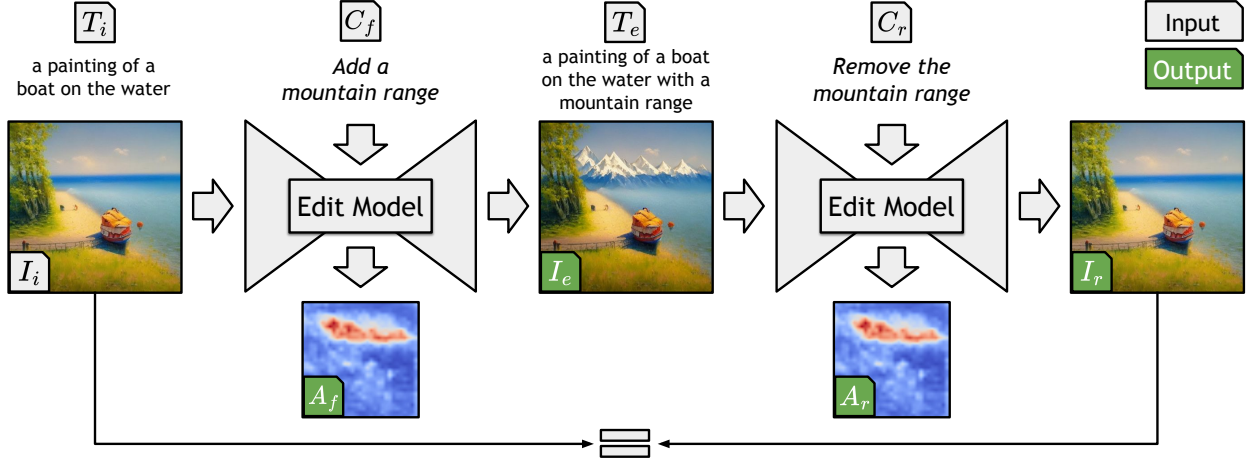


Figure 3. **Overview of the UIP2P training framework.** The model learns instruction-based image editing by applying forward and reverse instructions. Starting with an input image and a forward instruction, shared *Edit Model* generates an edited image. A reverse instruction is then applied to reconstruct the original image, enforcing Edit Reversibility Constraint (ERC).

4.1. Framework

4.1.1. UIP2P

To enforce the Edit Reversibility Constraint (ERC), we define each training step as a sequence of a forward edit followed by its corresponding reverse edit, both applied using the same *Edit Model*. This ensures that modifications can be undone accurately, embedding edit constraints directly within the training process, see Fig. 3 for an overview. A key advantage of our approach is that training is performed *in a single denoising step*, significantly reducing computational cost compared to existing methods that require multiple refinement passes per edit. To enforce the semantic correctness of ERC, we introduce three core components:

1. **Text and Image Direction Alignment:** We leverage CLIP embeddings [36] to align the semantic relationship between textual instructions and image modifications without the need of ground-truth edited images. By operating within CLIP’s embedding space, our model ensures that changes in the input and edited images correspond to changes in their respective captions. This alignment is critical for enforcing the Edit Reversibility Constraint (ERC), ensuring that edits accurately follow instructions while preserving the input image’s structure.
2. **Attention Map Alignment:** To ensure stable and well-localized edits, we enforce alignment between cross-attention maps generated during both forward and reverse edits. This ensures the model focuses on the same regions of the image when applying and undoing modifications. Attention Map Alignment also regularizes the training objective, improving spatial precision in edits.
3. **Reconstruction Alignment:** A key aspect of ERC is the ability to reconstruct the original input after applying the

reverse instruction. This ensures that the model reliably undoes its edits. We achieve this by minimizing both pixel-wise and semantic discrepancies between the reconstructed image and the original input, reinforcing the accuracy of the applied and reversed edits.

During training, we sample a *noise level* t from a pre-defined schedule and apply it to the input image, I_i , to obtain the noisy version. Based on the *forward instruction*, C_f , *Edit Model* then predicts and removes this noise to generate the *edited image*, I_e . The *reverse instruction*, C_r , is then applied, using another sampled noise level \hat{t} , to recover the original image, I_r . This *single-step training approach* ensures that ERC is learned efficiently across varying noise scales, improving robustness across diverse edit scenarios.

By combining these three components—Text and Image Direction Alignment, Attention Map Alignment, and Reconstruction Alignment—our framework enforces ERC on real-image datasets *without requiring triplets of input-edited images with edit instructions*. This enables our approach to scale effectively beyond synthetic datasets, making it a practical solution for real-world instruction-based image editing.

4.1.2. Loss Functions

To enforce ERC, we introduce loss terms that guide editing and reconstruction. Each training iteration processes a *single-step training* sample consisting of an input image, an edit instruction, a reverse instruction, and captions.

CLIP Direction Loss. This loss ensures that the transformation applied to the image aligns with the text instruction in CLIP’s semantic space [14]. Given the CLIP embeddings of the input image (E_{I_i}), edited image (E_{I_e}), input caption (E_{T_i}), and edited caption (E_{T_e}), the loss is defined as:

Table 1. **Reverse Instruction Generation.** Our method generates reverse instructions for the IP2P dataset, eliminating the need for ground-truth edited images. Additionally, edit instructions, edited captions, and reverse instructions are generated for CC3M and CC12M datasets—denoted as CCXM. The **texts** are generated by LLMs such as GEMINI, and GEMMA2.

	Input Caption	Edit Instruction	Edited Caption	Reverse Instruction
IP2P	A man wearing a denim jacket	make the jacket a rain coat	A man wearing a rain coat	make the coat a denim jacket
	A sofa in the living room	add pillows	A sofa in the living room with pillows	remove the pillows

CCXM	Person on the cover of a magazine	make the person a cat	Cat on the cover of the magazine	make the cat a person
	A tourist rests against a concrete wall	give him a backpack	A tourist with a backpack rests against a concrete wall	remove his backpack

$$\mathcal{L}_{\text{CLIP}} = 1 - \cos(E_{I_e} - E_{I_i}, E_{T_e} - E_{T_i}) \quad (1)$$

By aligning the direction of change in image space with the transformation described in text space, this loss ensures that modifications accurately reflect the intended semantic edits.

Attention Map Alignment Loss. To ensure that the same regions of the image are modified during both forward and reverse edits, we introduce an attention map alignment loss. Let $A_f^{(i)}$ and $A_r^{(i)}$ represent the cross-attention maps from the i -th layer of the U-Net model during the forward and reverse edits, respectively. The loss is defined as:

$$\mathcal{L}_{\text{attn}} = \sum_i \left\| A_f^{(i)} - A_r^{(i)} \right\|_2 \quad (2)$$

This loss ensures the model focuses on the same image regions during both forward and reverse edits—a key requirement for ERC. We compute it across U-Net’s down and up layers at random timesteps. By encouraging consistent cross-attention maps, the loss promotes spatial coherence across noise levels, as fixed instructions tend to yield stable attention over edited regions (see Supp. Sec. 4.2).

CLIP Similarity Loss. This loss encourages the edited image to remain semantically aligned with the provided textual instruction. It is calculated as the cosine similarity between the CLIP embeddings of the edited image (E_{I_e}) and the edited caption (E_{T_e}):

$$\mathcal{L}_{\text{sim}} = 1 - \cos(E_{I_e}, E_{T_e}) \quad (3)$$

This loss ensures that the generated image aligns with the intended edits, maintaining semantic alignment with the provided instructions.

Reconstruction Loss. To guarantee that the original image is recovered after the reverse edit, we employ a reconstruction loss consisting of a pixel-wise loss and a CLIP-based semantic loss. The total reconstruction loss is defined as:

$$\mathcal{L}_{\text{recon}} = \|I_i - I_r\|_2 + [1 - \cos(E_{I_i}, E_{I_r})] \quad (4)$$

This loss ensures that the model can accurately reverse edits and return to the original image when the reverse instruction is applied, enforcing ERC by minimizing differences between the input and reconstructed images.

Total Loss. Overall, all losses are applied to a *single-step noise prediction*, making training more efficient. It is defined as a weighted combination of the individual losses:

$$\mathcal{L}_{\text{ERC}} = \lambda_{\text{CLIP}} \mathcal{L}_{\text{CLIP}} + \lambda_{\text{attn}} \mathcal{L}_{\text{attn}} + \lambda_{\text{sim}} \mathcal{L}_{\text{sim}} + \lambda_{\text{recon}} \mathcal{L}_{\text{recon}} \quad (5)$$

where λ_{CLIP} , λ_{attn} , λ_{sim} , and λ_{recon} are parameters that control the relative contributions of each loss term. The weights are selected through validation-based grid search to minimize \mathcal{L}_{ERC} on a held-out set. Starting from the base configuration with $\mathcal{L}_{\text{CLIP}}$ and $\mathcal{L}_{\text{recon}}$, we found that \mathcal{L}_{sim} enables freer edits by encouraging stronger image-text alignment, while $\mathcal{L}_{\text{attn}}$ improves localization by focusing on relevant regions during both forward and reverse edits.

4.2. Training Data

To enable ERC training on datasets with image and edit instructions [6], we leverage Large Language Models (LLMs), such as GEMMA2 [49] and GEMINI [48], to automatically generate reverse edit instructions. These LLMs provide an efficient and scalable solution for obtaining reverse instructions with minimal cost and effort [6]. We use GEMINI to enrich the IP2P dataset with reverse instructions based on the input caption, edit instruction, and corresponding edited caption. To improve model performance, we employ few-shot prompting during this process, enabling the generation of reverse instructions without the need for manually paired datasets, which significantly enhances scalability. The reverse instructions generated by the LLM aim to revert the edited image to its original form (see Tab. 1 - IP2P section). Using the enriched dataset with reverse instructions (see Tab. 1, IP2P section), we fine-tune GEMMA2 [49], to generate an edit instruction, edited caption, and reverse instruction given an input caption. We use

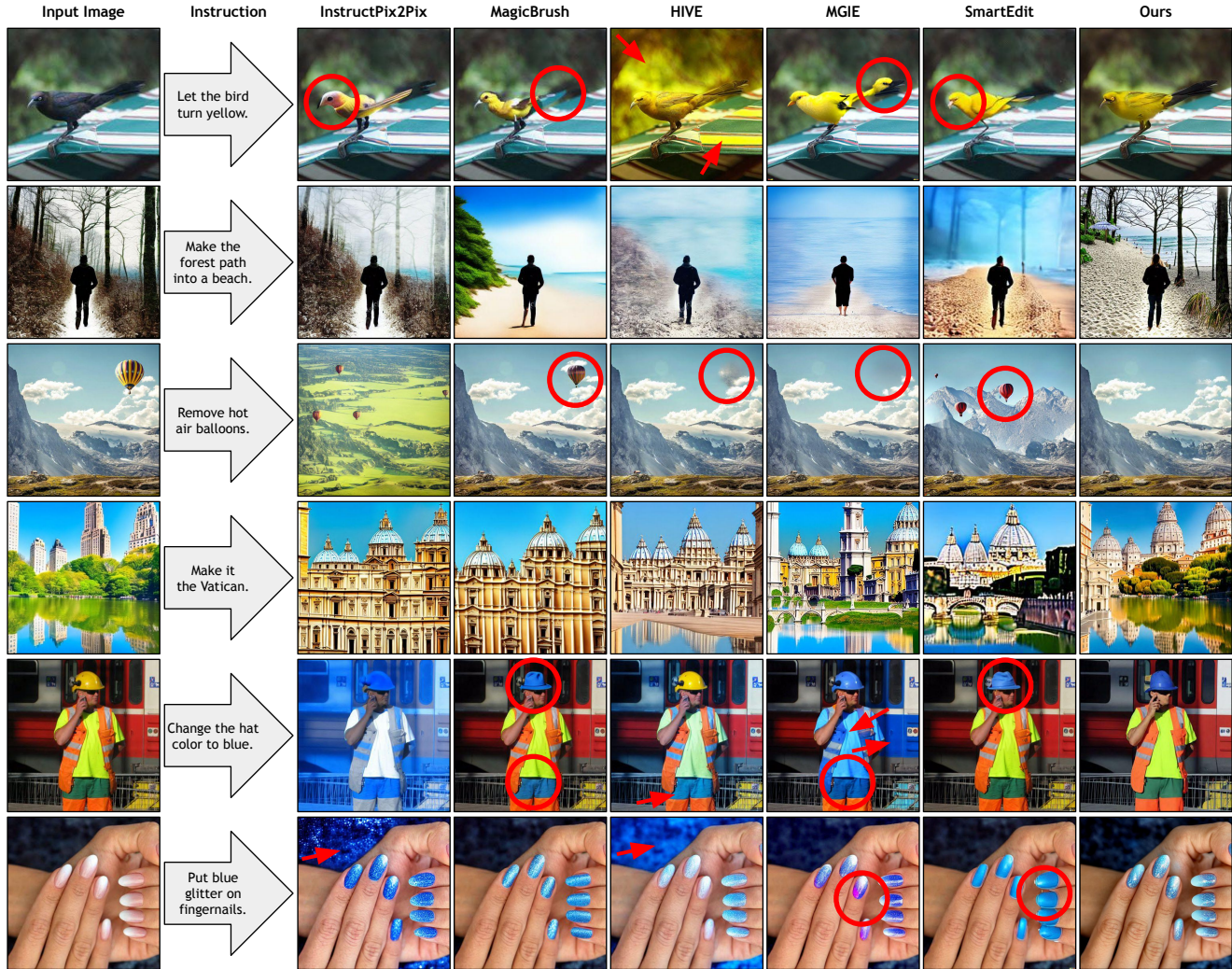


Figure 4. **Qualitative Examples.** UIP2P performance is shown across various tasks and datasets, compared to InstructPix2Pix, MagicBrush, HIVE, MGIE, and SmartEdit. Our method demonstrates either comparable or superior results in terms of accurately applying the requested edits while preserving visual consistency. Red circles and arrows indicate drastic problems during the image editing.

this fine-tuned model to allow training on image-caption paired datasets such as CC3M and CC12M [8, 42], generating forward and reverse edits along with corresponding edited captions (see Tab. 1, CCXM section).

5. Experiments

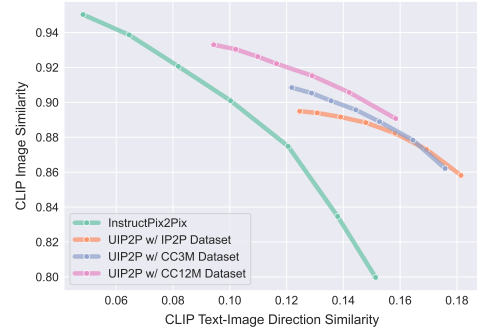
Datasets. We generate datasets consisting of forward and reverse instructions, as detailed in Sec. 4.2. For the initial experiments, we use the InstructPix2Pix dataset [6], which provides generated image-caption pairs along with edit instructions. We further extend our experiments to real-image datasets, including CC3M [42] and CC12M [8], for which we generate eight possible edits per image-caption pair. This increases diversity in the editing tasks, exposing the model to a wide range of transformations and enhancing

its ability to generalize across different types of edits and real-world scenarios. We then also conduct experiments on the HQ-Edit dataset [21], which already contains reverse instructions and higher-quality images, though they are still generated by off-the-shelf multimodal models [1, 4].

Baselines. We evaluate our method by comparing it against several models. The primary baseline is InstructPix2Pix [6], a supervised method that relies on ground-truth edited images during training. To demonstrate the advantages of our unsupervised approach, we train and test both IP2P and our model on the same datasets, with our method not using the ground-truth edited images while training. We also compare our method with other instruction-based editing models, including MagicBrush [58], HIVE [59], MGIE [12], SmartEdit [20], and HQ-Edit [21]. These comparisons allow us

Settings	Methods	L1↓	L2↓	CLIP-I↑	DINO↑	CLIP-T↑
Single-turn	HIVE [59]	0.1092	0.0341	0.8519	0.7500	0.2752
	InstructPix2Pix [6]	0.1122	0.0371	0.8524	0.7428	0.2764
	UIP2P w/ IP2P Dataset	0.0722	0.0193	0.9243	0.8876	0.2944
	UIP2P w/ HQ-Edit Dataset	0.0709	0.0190	0.9251	0.8882	0.2932
	UIP2P w/ CC3M Dataset	0.0680	0.0183	0.9262	0.8924	0.2966
	UIP2P w/ CC12M Dataset	0.0619	0.0174	0.9318	0.9039	0.2964
Multi-turn	HIVE [59]	0.1521	0.0557	0.8004	0.6463	0.2673
	InstructPix2Pix [6]	0.1584	0.0598	0.7924	0.6177	0.2726
	UIP2P w/ IP2P Dataset	0.1104	0.0358	0.8779	0.8041	0.2892
	UIP2P w/ HQ-Edit Dataset	0.1060	0.0344	0.8792	0.8081	0.2897
	UIP2P w/ CC3M Dataset	0.1040	0.0337	0.8816	0.8130	0.2909
	UIP2P w/ CC12M Dataset	0.0976	0.0323	0.8857	0.8235	0.2901

(a) **Zero-shot Quantitative Comparison on MagicBrush [58] test set.** Instruction-based editing methods that are not fine-tuned on MagicBrush are presented. In the multi-turn setting, target images are iteratively edited from the initial images.



(b) **Evaluation on the IP2P test dataset.** UIP2P outperforms IP2P in both CLIP image similarity and CLIP text-image similarity metrics, demonstrating better visual fidelity and instruction alignment.

Figure 5. Evaluation on MagicBrush and IP2P test datasets.

to evaluate how effectively our model handles diverse and complex edits without needing for editing methods to generate ground-truth edited images or human-annotated data.

Implementation Details. Our method, UIP2P, fine-tunes the SD-v1.5 checkpoint [39] without any pre-training on triplet datasets. While we retain the IP2P architecture (*Edit Model*, see Fig. 3), our approach employs different training objectives, focusing primarily on enforcing the ERC. Specifically, we leverage the CLIP ViT-L/14 model, already integrated into SD-v1.5, to compute the losses. Unlike supervised methods that begin training by adding noise to the ground-truth edited image, our method starts by adding noise to the input image. This design choice has significant implications, *e.g.*, it helps bias the model toward preserving the structure and details of the original image, ensuring that edits remain consistent with the input. Our method trains in a single denoising step, predicting only one step per iteration to ensure efficiency. UIP2P is trained using the AdamW optimizer [28] with a batch size of 256 over 11K iterations. The base learning rate is set to 1e-05. All experiments are conducted on 8 NVIDIA A100 GPUs, with loss weights set as $\lambda_{\text{CLIP}} = 1.0$, $\lambda_{\text{attn}} = 0.5$, $\lambda_{\text{sim}} = 1.0$, and $\lambda_{\text{recon}} = 1.0$. The best configuration is selected based on the validation loss of \mathcal{L}_{ERC} .

5.1. Qualitative Results

We compare UIP2P with state-of-the-art methods, including InstructPix2Pix [6], MagicBrush [58], HIVE [59], MGIE [12], and SmartEdit [20], on various datasets [6, 44, 45, 58]. The tasks include color modifications, object removal, and structural changes. UIP2P consistently produces high-quality edits, applying transformations accurately while maintaining visual coherence. For example, in “let the bird turn yellow,” UIP2P provides a more natural color change while preserving the bird’s shape. Similar improvements are observed in tasks like “remove hot air balloons” and “change hat color to blue.” These results

highlight UIP2P’s ability to perform diverse edits, achieving successful and localized image modifications (see Fig. 4).

5.2. Quantitative Results

5.2.1. IP2P Test Dataset

We evaluate our method on the IP2P test split, containing 5K image-instruction pairs. Following [6], we use CLIP image similarity for visual fidelity and CLIP text-image similarity to assess alignment with the instructions. Higher scores in both metrics indicate better performance (upper right corner) by preserving image details (image similarity) and effectively applying the edits (direction similarity). As shown in Fig. 5b, UIP2P outperforms IP2P across both metrics. In these experiments, the text scale s_T is fixed, while the image scale s_I varies from 1.0 to 2.2.

5.2.2. MagicBrush Test Dataset

The MagicBrush test split contains 535 sessions (source images for iterative editing) and 1053 turns (individual editing steps). It uses L1 and L2 norms for pixel accuracy, CLIP-I and DINO embeddings for image quality via cosine similarity, and CLIP-T to ensure alignment with local text descriptions. As seen in Fig. 5a, UIP2P performs the best for both single- and multi-turn settings. It is important to be noted that HIVE utilizes human feedback on edited images to understand user preferences and fine-tunes IP2P based on learned rewards, aligning the model more closely with human expectations. Figure 5a shows that adding inverse instructions to IP2P improves performance, while training on HQ-Edit further enhances results due to its high-quality/resolution images and built-in reverse instructions. However, its smaller size ($\approx 100\text{K}$) and specialized collection pipeline limit its impact. In contrast, leveraging large-scale real-image datasets like CC3M and CC12M enables scalable training without labor-intensive data collection, achieving the best overall performance. See Appendix for more quantitative comparison.

5.2.3. User Study

We conduct a user study on the Prolific platform [35] with 50 participants to evaluate six methods—IP2P, MagicBrush, HIVE, MGIE, SmartEdit, and UIP2P—on 30 randomly sampled image-edit instructions from diverse datasets [6, 44, 45, 58]. Participants compare images from randomly paired methods, selecting the better-performing one across six pairs per question, yielding 18,000 total votes—9,000 for *edit success* and 9,000 for *localization accuracy*. In two runs, they first choose the model best following the instruction, *Successful*, then the one applying edits only to the intended area, *Localized*. To ensure robust evaluation, we use *Elo rating system* [11], a widely adopted ranking method in LLM and generative model benchmarking [5, 61]. By enabling continuous pairwise comparisons, Elo accounts for varying instruction difficulty and produces a relative ranking. Table 2 shows that UIP2P achieves the highest *Elo score* and adjusted *Win rate* across both criteria. See Appendix for more details.

Table 2. **User study.** Results comparing six methods based on Elo scores and top performer ratios for edit success and localization accuracy. UIP2P achieves the highest scores in both criteria.

Models	Successful		Localized	
	Elo score	Win rate	Elo score	Win rate
IP2P	1395	12%	1301	12%
MagicBrush	1482	16%	<u>1601</u>	<u>18%</u>
HIVE	1465	15%	1471	14%
MGIE	<u>1584</u>	<u>18%</u>	1529	17%
SmartEdit	1543	17%	1440	16%
UIP2P (Ours)	1681	22%	1659	23%

5.3. Ablation Study

Scalability. We train our method on IP2P, HQ-Edit, CC3M, and CC12M to assess its scalability with dataset size and quality. As shown in Fig. 5a, performance improves with larger and higher-quality datasets, with notable gains from IP2P to CC12M. This highlights our method’s ability to leverage extensive data for better fidelity and localization. See Appendix for the discussion on runtime of our method.

Loss functions. We conduct a zero-shot evaluation on the MagicBrush test set (single-turn) to assess the contribution of each loss function, see Tab. 3 - Loss. Starting with the base configuration, containing \mathcal{L}_{CLIP} and \mathcal{L}_{recon} , we observe moderate performance across the same metrics. Adding \mathcal{L}_{sim} loss allows the model to perform edits more freely, as the *Base* without it tends to create outputs similar to the input image. Finally, \mathcal{L}_{attn} enhances the model’s focus on relevant regions and ensures that the region will remain consistent between the forward and reverse processes.

Attention Map Alignment Loss vs. Timestamp t . We compare the impact of using random timestamps t versus

Table 3. **Ablation studies.** Adding additional loss functions to the base setup improves performance on the MagicBrush benchmark. Additionally, using random timestamps between forward and reverse instructions leads to better edit localization and overall performance.

	Ablation	L1↓	L2↓	CLIP-I↑	DINO↑	CLIP-T↑
	IP2P [6]	0.112	0.037	0.852	0.743	0.276
Loss	Base	0.117	0.032	0.878	0.806	0.309
	+ \mathcal{L}_{sim}	0.089	0.024	0.906	0.872	0.301
	+ \mathcal{L}_{attn}	0.062	0.017	0.932	0.904	0.296
Attn	Same t	0.074	0.022	0.921	0.889	0.299
	Random t	0.062	0.017	0.932	0.904	0.296

same timestamps t between forward and reverse instructions. As shown in Tab. 3 - Attn, using random t consistently outperforms the fixed approach across all metrics. This suggests that introducing variability in t during training leads to a more consistent cross-attention, resulting in better edit localization and overall performance. The rationale is that using different noise levels enhances robustness by exposing the model to varied denoising conditions during forward and reverse edits, while the attention consistency loss ensures the model maintains focus on the same regions regardless of the noise level. As also investigated in [16, 46], maintaining consistent attention maps across different timestamps enables more precise editing.

6. Conclusion

In this work, we introduce UIP2P, a novel unsupervised approach for instruction-based image editing that eliminates the need for paired supervision through the ERC. By enabling training on real-image datasets, our approach enhances scalability while maintaining high-fidelity edits. Through a single-step training paradigm, we achieve efficient and precise edits, outperforming existing methods. While our method advances instruction-based editing, future improvements in reverse instruction generation, spatial guidance, and diffusion model efficiency can further enhance performance. Additionally, incorporating perceptual or adversarial losses could improve photorealism, addressing cases where optimizing for CLIP alignment may compromise visual quality in challenging edits. As models continue to evolve, our approach stands to benefit from these advancements, further improving edit precision and inference speed. Overall, our work unlocks new possibilities for large-scale training in instruction-based image editing without explicit supervision. We encourage future research to build upon this foundation, refining both model design and training strategies.

References

- [1] Josh Achiam, Steven Adler, Sandhini Agarwal, Lama Ahmad, Ilge Akkaya, Florencia Leoni Aleman, Diogo Almeida, Janko Altenschmidt, Sam Altman, Shyamal Anadkat, et al. Gpt-4 technical report. *arXiv preprint arXiv:2303.08774*, 2023. 2, 6
- [2] Omri Avrahami, Dani Lischinski, and Ohad Fried. Blended diffusion for text-driven editing of natural images. In *IEEE/CVF Conference on Computer Vision and Pattern Recognition, CVPR 2022, New Orleans, LA, USA, June 18-24, 2022*, pages 18187–18197. IEEE, 2022. 1
- [3] Omer Bar-Tal, Dolev Ofri-Amar, Rafail Fridman, Yoni Kasten, and Tali Dekel. Text2live: Text-driven layered image and video editing. In *Computer Vision - ECCV 2022 - 17th European Conference, Tel Aviv, Israel, October 23-27, 2022, Proceedings, Part XV*, pages 707–723. Springer, 2022. 15
- [4] James Betker, Gabriel Goh, Li Jing, Tim Brooks, Jianfeng Wang, Linjie Li, Long Ouyang, Juntang Zhuang, Joyce Lee, Yufei Guo, et al. Improving image generation with better captions. *Computer Science*. <https://cdn.openai.com/papers/dall-e-3.pdf>, 2(3):8, 2023. 2, 6
- [5] Meriem Boubdir, Edward Kim, Beyza Ermis, Sara Hooker, and Marzieh Fadaee. Elo uncovered: Robustness and best practices in language model evaluation. *arXiv preprint arXiv:2311.17295*, 2023. 8
- [6] Tim Brooks, Aleksander Holynski, and Alexei A. Efros. Instructpix2pix: Learning to follow image editing instructions. In *CVPR*, 2023. 1, 2, 3, 5, 6, 7, 8, 15, 17
- [7] Tom B. Brown, Benjamin Mann, Nick Ryder, Melanie Subbiah, Jared Kaplan, Prafulla Dhariwal, Arvind Neelakantan, Pranav Shyam, Girish Sastry, Amanda Askell, Sandhini Agarwal, Ariel Herbert-Voss, Gretchen Krueger, Tom Henighan, Rewon Child, Aditya Ramesh, Daniel M. Ziegler, Jeffrey Wu, Clemens Winter, Christopher Hesse, Mark Chen, Eric Sigler, Mateusz Litwin, Scott Gray, Benjamin Chess, Jack Clark, Christopher Berner, Sam McCandlish, Alec Radford, Ilya Sutskever, and Dario Amodei. Language models are few-shot learners. In *Advances in Neural Information Processing Systems 33: Annual Conference on Neural Information Processing Systems 2020, NeurIPS 2020, December 6-12, 2020, virtual*, 2020. 3
- [8] Soravit Changpinyo, Piyush Sharma, Nan Ding, and Radu Soricut. Conceptual 12m: Pushing web-scale image-text pre-training to recognize long-tail visual concepts. In *Proceedings of the IEEE/CVF conference on computer vision and pattern recognition*, pages 3558–3568, 2021. 6, 17
- [9] Guillaume Couairon, Jakob Verbeek, Holger Schwenk, and Matthieu Cord. Diffedit: Diffusion-based semantic image editing with mask guidance. In *The Eleventh International Conference on Learning Representations*, 2023. 1, 3
- [10] Katherine Crowson, Stella Biderman, Daniel Kornis, Dashiell Stander, Eric Hallahan, Louis Castricato, and Edward Raff. VQGAN-CLIP: open domain image generation and editing with natural language guidance. In *Computer Vision - ECCV 2022 - 17th European Conference, Tel Aviv, Israel, October 23-27, 2022, Proceedings, Part XXXVII*, pages 88–105. Springer, 2022. 15
- [11] Arpad Elo. *The Rating of Chess Players, Past and Present*. Batsford London, 1978. 8
- [12] Tsu-Jui Fu, Wenze Hu, Xianzhi Du, William Yang Wang, Yinfei Yang, and Zhe Gan. Guiding instruction-based image editing via multimodal large language models. *arXiv preprint arXiv:2309.17102*, 2023. 1, 2, 3, 6, 7, 12, 18
- [13] Rinon Gal, Yuval Alaluf, Yuval Atzmon, Or Patashnik, Amit H. Bermano, Gal Chechik, and Daniel Cohen-Or. An image is worth one word: Personalizing text-to-image generation using textual inversion, 2022. 1
- [14] Rinon Gal, Or Patashnik, Haggai Maron, Amit H. Bermano, Gal Chechik, and Daniel Cohen-Or. Stylegan-nada: Clip-guided domain adaptation of image generators. *ACM Trans. Graph.*, 41(4):141:1–141:13, 2022. 3, 4
- [15] Zigang Geng, Binxin Yang, Tiankai Hang, Chen Li, Shuyang Gu, Ting Zhang, Jianmin Bao, Zheng Zhang, Han Hu, Dong Chen, et al. Instructdiffusion: A generalist modeling interface for vision tasks. *arXiv preprint arXiv:2309.03895*, 2023. 3
- [16] Qin Guo and Tianwei Lin. Focus on your instruction: Fine-grained and multi-instruction image editing by attention modulation. In *Proceedings of the IEEE/CVF Conference on Computer Vision and Pattern Recognition*, pages 6986–6996, 2024. 8, 13
- [17] Amir Hertz, Ron Mokady, Jay Tenenbaum, Kfir Aberman, Yael Pritch, and Daniel Cohen-Or. Prompt-to-prompt image editing with cross attention control. *CoRR*, abs/2208.01626, 2022. 1, 2, 3, 17
- [18] Jonathan Ho and Tim Salimans. Classifier-free diffusion guidance. In *NeurIPS 2021 Workshop on Deep Generative Models and Downstream Applications*, 2021. 3
- [19] Jonathan Ho, Ajay Jain, and Pieter Abbeel. Denoising diffusion probabilistic models. *Advances in neural information processing systems*, 33:6840–6851, 2020. 1
- [20] Yuzhou Huang, Liangbin Xie, Xintao Wang, Ziyang Yuan, Xiaodong Cun, Yixiao Ge, Jiantao Zhou, Chao Dong, Rui Huang, Ruimao Zhang, et al. Smartedit: Exploring complex instruction-based image editing with multimodal large language models. In *Proceedings of the IEEE/CVF Conference on Computer Vision and Pattern Recognition*, pages 8362–8371, 2024. 1, 3, 6, 7, 12, 18
- [21] Mude Hui, Siwei Yang, Bingchen Zhao, Yichun Shi, Heng Wang, Peng Wang, Cihang Xie, and Yuyin Zhou. HQ-edit: A high-quality dataset for instruction-based image editing. In *The Thirteenth International Conference on Learning Representations*, 2025. 1, 2, 3, 6
- [22] Xuan Ju, Ailing Zeng, Yuxuan Bian, Shaoteng Liu, and Qiang Xu. Direct inversion: Boosting diffusion-based editing with 3 lines of code. *arXiv preprint arXiv:2310.01506*, 2023. 3, 14
- [23] Bahjat Kawar, Shiran Zada, Oran Lang, Omer Tov, Huiwen Chang, Tali Dekel, Inbar Mosseri, and Michal Irani. Imagic: Text-based real image editing with diffusion models. *CoRR*, abs/2210.09276, 2022. 1
- [24] Krishnamurthy Kenthapadi, Himabindu Lakkaraju, and Nazneen Rajani. Generative ai meets responsible ai: Practical challenges and opportunities. In *Proceedings of the 29th*

- ACM SIGKDD Conference on Knowledge Discovery and Data Mining*, pages 5805–5806, 2023. 12
- [25] Gwanghyun Kim, Taesung Kwon, and Jong Chul Ye. Diffusionclip: Text-guided diffusion models for robust image manipulation. In *Proceedings of the IEEE/CVF conference on computer vision and pattern recognition*, pages 2426–2435, 2022. 2, 3, 18
- [26] Pavel Korshunov and Sébastien Marcel. Deepfakes: a new threat to face recognition? assessment and detection. *arXiv preprint arXiv:1812.08685*, 2018. 12
- [27] Xihui Liu, Zhe Lin, Jianming Zhang, Handong Zhao, Quan Tran, Xiaogang Wang, and Hongsheng Li. Open-edit: Open-domain image manipulation with open-vocabulary instructions. In *Computer Vision - ECCV 2020 - 16th European Conference, Glasgow, UK, August 23-28, 2020, Proceedings, Part XI*, pages 89–106. Springer, 2020. 15
- [28] I Loshchilov. Decoupled weight decay regularization. *arXiv preprint arXiv:1711.05101*, 2017. 7
- [29] Andreas Lugmayr, Martin Danelljan, Andrés Romero, Fisher Yu, Radu Timofte, and Luc Van Gool. Repaint: Inpainting using denoising diffusion probabilistic models. In *IEEE/CVF Conference on Computer Vision and Pattern Recognition, CVPR 2022, New Orleans, LA, USA, June 18-24, 2022*, pages 11451–11461. IEEE, 2022. 1
- [30] Chenlin Meng, Yutong He, Yang Song, Jiaming Song, Jiajun Wu, Jun-Yan Zhu, and Stefano Ermon. SDEdit: Guided image synthesis and editing with stochastic differential equations. In *International Conference on Learning Representations*, 2022. 1, 3, 15
- [31] Ron Mokady, Amir Hertz, Kfir Aberman, Yael Pritch, and Daniel Cohen-Or. Null-text inversion for editing real images using guided diffusion models. *CoRR*, abs/2211.09794, 2022. 3, 15
- [32] Alexander Quinn Nichol, Prafulla Dhariwal, Aditya Ramesh, Pranav Shyam, Pamela Mishkin, Bob McGrew, Ilya Sutskever, and Mark Chen. GLIDE: towards photorealistic image generation and editing with text-guided diffusion models. In *International Conference on Machine Learning, 2022*, pages 16784–16804. PMLR, 2022. 1
- [33] Gaurav Parmar, Krishna Kumar Singh, Richard Zhang, Yijun Li, Jingwan Lu, and Jun-Yan Zhu. Zero-shot image-to-image translation. In *ACM SIGGRAPH 2023 Conference Proceedings*, pages 1–11, 2023. 3
- [34] Or Patashnik, Zongze Wu, Eli Shechtman, Daniel Cohen-Or, and Dani Lischinski. Styleclip: Text-driven manipulation of stylegan imagery. In *Proceedings of the IEEE/CVF International Conference on Computer Vision*, pages 2085–2094, 2021. 3
- [35] prolific. Prolific. <https://www.prolific.com/>, 2025. Accessed: 2025-03-01. 8
- [36] Alec Radford, Jong Wook Kim, Chris Hallacy, Aditya Ramesh, Gabriel Goh, Sandhini Agarwal, Girish Sastry, Amanda Askell, Pamela Mishkin, Jack Clark, Gretchen Krueger, and Ilya Sutskever. Learning transferable visual models from natural language supervision. In *Proceedings of the 38th International Conference on Machine Learning, 2021*, pages 8748–8763. PMLR, 2021. 4, 17
- [37] Alec Radford, Jong Wook Kim, Chris Hallacy, Aditya Ramesh, Gabriel Goh, Sandhini Agarwal, Girish Sastry, Amanda Askell, Pamela Mishkin, Jack Clark, Gretchen Krueger, and Ilya Sutskever. Learning transferable visual models from natural language supervision. In *Proceedings of the 38th International Conference on Machine Learning*, pages 8748–8763, 2021. 2
- [38] Aditya Ramesh, Prafulla Dhariwal, Alex Nichol, Casey Chu, and Mark Chen. Hierarchical text-conditional image generation with CLIP latents. *CoRR*, abs/2204.06125, 2022. 1
- [39] Robin Rombach, Andreas Blattmann, Dominik Lorenz, Patrick Esser, and Björn Ommer. High-resolution image synthesis with latent diffusion models. In *IEEE/CVF Conference on Computer Vision and Pattern Recognition, 2022*, pages 10674–10685. IEEE, 2022. 1, 3, 7
- [40] Nataniel Ruiz, Yuanzhen Li, Varun Jampani, Yael Pritch, Michael Rubinstein, and Kfir Aberman. Dreambooth: Fine tuning text-to-image diffusion models for subject-driven generation. In *Proceedings of the IEEE/CVF Conference on Computer Vision and Pattern Recognition (CVPR)*, pages 22500–22510, 2023. 1
- [41] Chitwan Saharia, William Chan, Saurabh Saxena, Lala Li, Jay Whang, Emily Denton, Seyed Kamyar Seyed Ghasemipour, Raphael Gontijo-Lopes, Burcu Karagol Ayan, Tim Salimans, Jonathan Ho, David J. Fleet, and Mohammad Norouzi. Photorealistic text-to-image diffusion models with deep language understanding. In *Advances in Neural Information Processing Systems*, 2022. 1
- [42] Piyush Sharma, Nan Ding, Sebastian Goodman, and Radu Soricut. Conceptual captions: A cleaned, hypernymed, image alt-text dataset for automatic image captioning. In *Proceedings of the 56th Annual Meeting of the Association for Computational Linguistics (Volume 1: Long Papers)*, pages 2556–2565, 2018. 6, 17
- [43] Shelly Sheynin, Adam Polyak, Uriel Singer, Yuval Kirstain, Amit Zohar, Oron Ashual, Devi Parikh, and Yaniv Taigman. Emu edit: Precise image editing via recognition and generation tasks. *arXiv preprint arXiv:2311.10089*, 2023. 15
- [44] Jing Shi, Ning Xu, Trung Bui, Franck Dérnoncourt, Zheng Wen, and Chenliang Xu. A benchmark and baseline for language-driven image editing. In *Computer Vision - ACCV 2020 - 15th Asian Conference on Computer Vision, Kyoto, Japan, November 30 - December 4, 2020, Revised Selected Papers, Part VI*, pages 636–651. Springer, 2020. 7, 8
- [45] Jing Shi, Ning Xu, Yihang Xu, Trung Bui, Franck Dérnoncourt, and Chenliang Xu. Learning by planning: Language-guided global image editing. In *Proceedings of the IEEE/CVF Conference on Computer Vision and Pattern Recognition*, pages 13590–13599, 2021. 7, 8
- [46] Enis Simsar, Alessio Tonioni, Yongqin Xian, Thomas Hofmann, and Federico Tombari. Lime: Localized image editing via attention regularization in diffusion models. In *Proceedings of the Winter Conference on Applications of Computer Vision (WACV)*, pages 222–231, 2025. 8, 13
- [47] Xuan Su, Jiaming Song, Chenlin Meng, and Stefano Ermon. Dual diffusion implicit bridges for image-to-image translation. *arXiv preprint arXiv:2203.08382*, 2022. 2, 3

- [48] Gemini Team, Rohan Anil, Sebastian Borgeaud, Yonghui Wu, Jean-Baptiste Alayrac, Jiahui Yu, Radu Soricut, Johan Schalkwyk, Andrew M Dai, Anja Hauth, et al. Gemini: a family of highly capable multimodal models. *arXiv preprint arXiv:2312.11805*, 2023. 5
- [49] Gemma Team, Morgane Riviere, Shreya Pathak, Pier Giuseppe Sessa, Cassidy Hardin, Surya Bhupatiraju, Léonard Hussenot, Thomas Mesnard, Bobak Shahriari, Alexandre Ramé, et al. Gemma 2: Improving open language models at a practical size. *arXiv preprint arXiv:2408.00118*, 2024. 5
- [50] Narek Tumanyan, Michal Geyer, Shai Bagon, and Tali Dekel. Plug-and-play diffusion features for text-driven image-to-image translation. In *Proceedings of the IEEE/CVF Conference on Computer Vision and Pattern Recognition*, pages 1921–1930, 2023. 15
- [51] Kai Wang, Fei Yang, Shiqi Yang, Muhammad Atif Butt, and Joost van de Weijer. Dynamic prompt learning: Addressing cross-attention leakage for text-based image editing. In *Thirty-seventh Conference on Neural Information Processing Systems*, 2023. 3
- [52] Qian Wang, Biao Zhang, Michael Birsak, and Peter Wonka. Mdp: A generalized framework for text-guided image editing by manipulating the diffusion path, 2023. 3
- [53] Yuxiang Wei, Yabo Zhang, Zhilong Ji, Jinfeng Bai, Lei Zhang, and Wangmeng Zuo. Elite: Encoding visual concepts into textual embeddings for customized text-to-image generation. *arXiv preprint arXiv:2302.13848*, 2023. 1
- [54] Chen Henry Wu and Fernando De la Torre. A latent space of stochastic diffusion models for zero-shot image editing and guidance. In *ICCV*, 2023. 2, 3
- [55] Qiucheng Wu, Yujian Liu, Handong Zhao, Ajinkya Kale, Trung Bui, Tong Yu, Zhe Lin, Yang Zhang, and Shiyu Chang. Uncovering the disentanglement capability in text-to-image diffusion models. In *Proceedings of the IEEE/CVF Conference on Computer Vision and Pattern Recognition*, pages 1900–1910, 2023. 3
- [56] Sihan Xu, Ziqiao Ma, Yidong Huang, Honglak Lee, and Joyce Chai. Cyclenet: Rethinking cycle consistent in text-guided diffusion for image manipulation. In *Advances in Neural Information Processing Systems (NeurIPS)*, 2023. 2, 3
- [57] Binxin Yang, Shuyang Gu, Bo Zhang, Ting Zhang, Xuejin Chen, Xiaoyan Sun, Dong Chen, and Fang Wen. Paint by example: Exemplar-based image editing with diffusion models. In *Proceedings of the IEEE/CVF Conference on Computer Vision and Pattern Recognition*, pages 18381–18391, 2023. 1
- [58] Kai Zhang, Lingbo Mo, Wenhui Chen, Huan Sun, and Yu Su. Magicbrush: A manually annotated dataset for instruction-guided image editing. In *Advances in Neural Information Processing Systems*, 2023. 1, 2, 3, 6, 7, 8, 15, 17, 18
- [59] Shu Zhang, Xinyi Yang, Yihao Feng, Can Qin, Chia-Chih Chen, Ning Yu, Zeyuan Chen, Huan Wang, Silvio Savarese, Stefano Ermon, Caiming Xiong, and Ran Xu. HIVE: harnessing human feedback for instructional visual editing. *CoRR*, abs/2303.09618, 2023. 1, 2, 3, 6, 7, 15, 18
- [60] Haozhe Zhao, Xiaojuan Shawn Ma, Liang Chen, Shuzheng Si, Rujie Wu, Kaikai An, Peiyu Yu, Minjia Zhang, Qing Li, and Baobao Chang. Ultraedit: Instruction-based fine-grained image editing at scale. *Advances in Neural Information Processing Systems*, 37:3058–3093, 2024. 3
- [61] Lianmin Zheng, Ying Sheng, Wei-Lin Chiang, Hao Zhang, Joseph E Gonzalez, and Ion Stoica. Chatbot arena: benchmarking llms in the wild with elo ratings. *LMSYS Org. URL: https://lmsys.org/blog/2023-05-03-arena* [accessed 2024-04-16], 2023. 8
- [62] Jun-Yan Zhu, Taesung Park, Phillip Isola, and Alexei A. Efros. Unpaired image-to-image translation using cycle-consistent adversarial networks. In *IEEE International Conference on Computer Vision, ICCV 2017, Venice, Italy, October 22-29, 2017*, pages 2242–2251. IEEE Computer Society, 2017. 2

Table of Contents

A Ethics Statement	12
B Runtime Analysis	12
C Elo Rating System	12
C.1. Implementation Details	12
C.2. Interpreting Elo Scores	12
D Additional Details on Ablation Studies	13
D.1. Loss Functions	13
D.2. Attention Across Noise Steps in Training	13
E Additional Qualitative Results	13
F. Additional Quantitative Results	14
F.1. Evaluation on PIE-Bench	14
F.2. Evaluation on Emu Edit	15
F.3. Evaluation on MagicBrush Test	15
G Edit Reversibility Constraint Example	15
H Dataset Details	15
H.1. LLM Prompts for Data Generation	15
H.2. Dataset Filtering	17
H.3. More Examples from Reverse Instructions Dataset	17
I. Additional Implementation Details	17
I.1. Details of Competitor Methods	17
I.2. Code Implementation Overview	18
I.3. Algorithm Overview	18
J. Limitations and Failure Cases	18

A. Ethics Statement

Advancements in localized image editing technology offer substantial opportunities to enhance creative expression and improve accessibility within digital media and virtual reality environments. Nonetheless, these developments also bring forth important ethical challenges, particularly concerning the misuse of such technology to create misleading content, such as deepfakes [26], and its potential effect on employment in the image editing industry. Moreover, as also highlighted by [24], it requires a thorough and careful discussion about their ethical use to avoid possible misuse. We believe that our method could help reduce some of the biases present in previous datasets, though it will still be affected by biases inherent in models such as CLIP. Ethical frameworks should prioritize encouraging responsible usage, developing clear guidelines to prevent misuse, and promoting fairness and transparency, particularly in sensitive contexts like journalism. Effectively addressing these

concerns is crucial to amplifying the positive benefits of the technology while minimizing associated risks. In addition, our user study follows strict anonymity rules to protect the privacy of participants.

B. Runtime Analysis

Our method modifies the training objectives of IP2P by incorporating Edit Reversibility Constraint (ERC) and additional loss functions. However, these changes do not affect the overall runtime. Inference time remains comparable to the original IP2P framework, as we retain the same architecture and model structure. Consequently, our approach introduces no additional complexity or overhead in terms of processing time or resource consumption. This gives UIP2P an advantage over methods like MGIE [12] and SmartEdit [20], which rely on large language models (LLMs) during inference in terms of runtime and resource consumption.

C. Elo Rating System

The Elo rating system is a widely used method for ranking competitors in pairwise comparisons, originally designed for chess and later adopted in various domains, including generative model evaluation. It assigns each candidate a score that dynamically updates based on comparative performance. A higher Elo score indicates stronger performance relative to other candidates.

C.1. Implementation Details

Our implementation follows the standard Elo rating mechanism with the following key components:

- **Initial Rating:** Each model starts with a rating of **1500**.
- **K-Factor** ($K = 32$): Governs the magnitude of rating updates.
- **Expected Score Calculation:** The probability of a model winning against another is computed as:

$$E_A = \frac{1}{1 + 10^{(R_B - R_A)/400}} \quad (6)$$

where R_A and R_B are the Elo ratings of the two competing models.

- **Score Update Rule:** After each comparison, the winner’s rating increases, and the loser’s rating decreases:

$$R'_A = R_A + K(S_A - E_A) \quad (7)$$

where $S_A = 1$ for a win, 0 for a loss, and 0.5 for a draw.

C.2. Interpreting Elo Scores

Elo scores provide an intuitive understanding of model performance:

- **Higher Scores:** Indicate models that consistently outperform others.

- **Score Differences:** A gap of 400 points implies the higher-rated model is **10 times more likely** to win.
- **Stability of Rankings:** As the number of votes increases, the Elo system converges, producing a reliable performance ranking.

By leveraging the Elo rating system, we ensure a **robust, adaptive, and comparative** evaluation framework for image-editing models. This approach provides a dynamic ranking that accounts for dataset variations and human annotation biases, aligning with best practices in benchmarking generative models.

D. Additional Details on Ablation Studies

D.1. Loss Functions



Figure 6. **Visual effects of loss components.** This figure demonstrates how different loss components affect the final editing results. The comparison shows the impact of various loss terms on edit quality and localization.

We focused our ablation studies on \mathcal{L}_{sim} and \mathcal{L}_{attn} because these losses are additional components beyond the core \mathcal{L}_{CLIP} and \mathcal{L}_{recon} . The core losses are essential for ensuring semantic alignment and reversibility in Edit Reversibility Constraint (ERC), forming the foundation of our method. Without \mathcal{L}_{CLIP} and \mathcal{L}_{recon} , the model risks diverging, losing its ability to preserve both the input’s structure and its semantic coherence during edits.

Adding \mathcal{L}_{sim} enables the model to perform edits more freely by encouraging alignment between image and textual embeddings, thereby expanding its capacity for complex and diverse transformations. On the other hand, \mathcal{L}_{attn} refines the model’s ability to focus on relevant regions during edits, improving localization and reducing unintended changes in non-targeted areas.

\mathcal{L}_{CLIP} is applied between the input image and the edited image to ensure semantic alignment with the edit instruction. The reconstructed image is already constrained by \mathcal{L}_{recon} , which enforces structural and semantic consistency with the input. Adding \mathcal{L}_{CLIP} to the reconstructed image would be redundant and could interfere with the reversibility objective. Our design does not apply \mathcal{L}_{CLIP} to the reconstructed image to preserve the focus on reversibility and prevent conflicting optimization objectives.

D.2. Attention Across Noise Steps in Training

At training time, we sample two different noise steps for the

forward and backward processes, which are conditioned on the input image and edit instruction. Attention consistency is enforced between these different noise steps to ensure that the model attends to the same regions during both forward and reverse edits. This is supported by the observation that cross-attention scores in instruction-based editing methods tend to be more consistent across timesteps, as the edit instruction remains fixed and the model’s focus shifts only to the regions being edited (see Fig. 7).

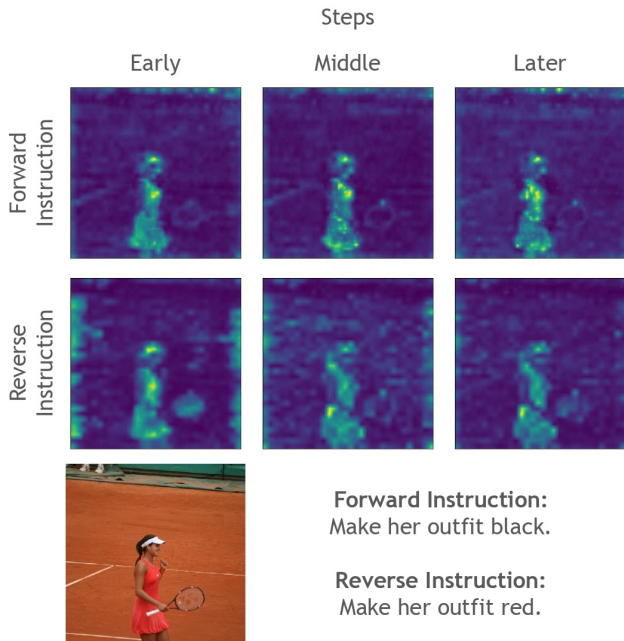


Figure 7. **Attention maps for diffusion steps.** Cross-attention maps for forward (top) and reverse (middle) instructions across early, middle, and later noise steps. The model enforces attention consistency, focusing on relevant regions for both edits.

Recent works, such as those by Guo et al. [16] and Simsar et al. [46], demonstrate that regularizing attention space with a mask during inference enables localized edits in IP2P. Our method builds on these ideas by incorporating attention consistency into the training phase, making it possible to focus on relevant regions from the start and avoiding the need for additional inference-time modifications.

E. Additional Qualitative Results

To further demonstrate the capabilities of our approach, we present additional qualitative comparisons in Fig. 8. These results showcase the performance of our method against several baseline models, including InstructPix2Pix, MagicBrush, HIVE, MGIE, and SmartEdit, across a diverse set of editing instructions. These tasks range from simple edits, such as color adjustments and expression changes, to more challenging transformations, including object re-

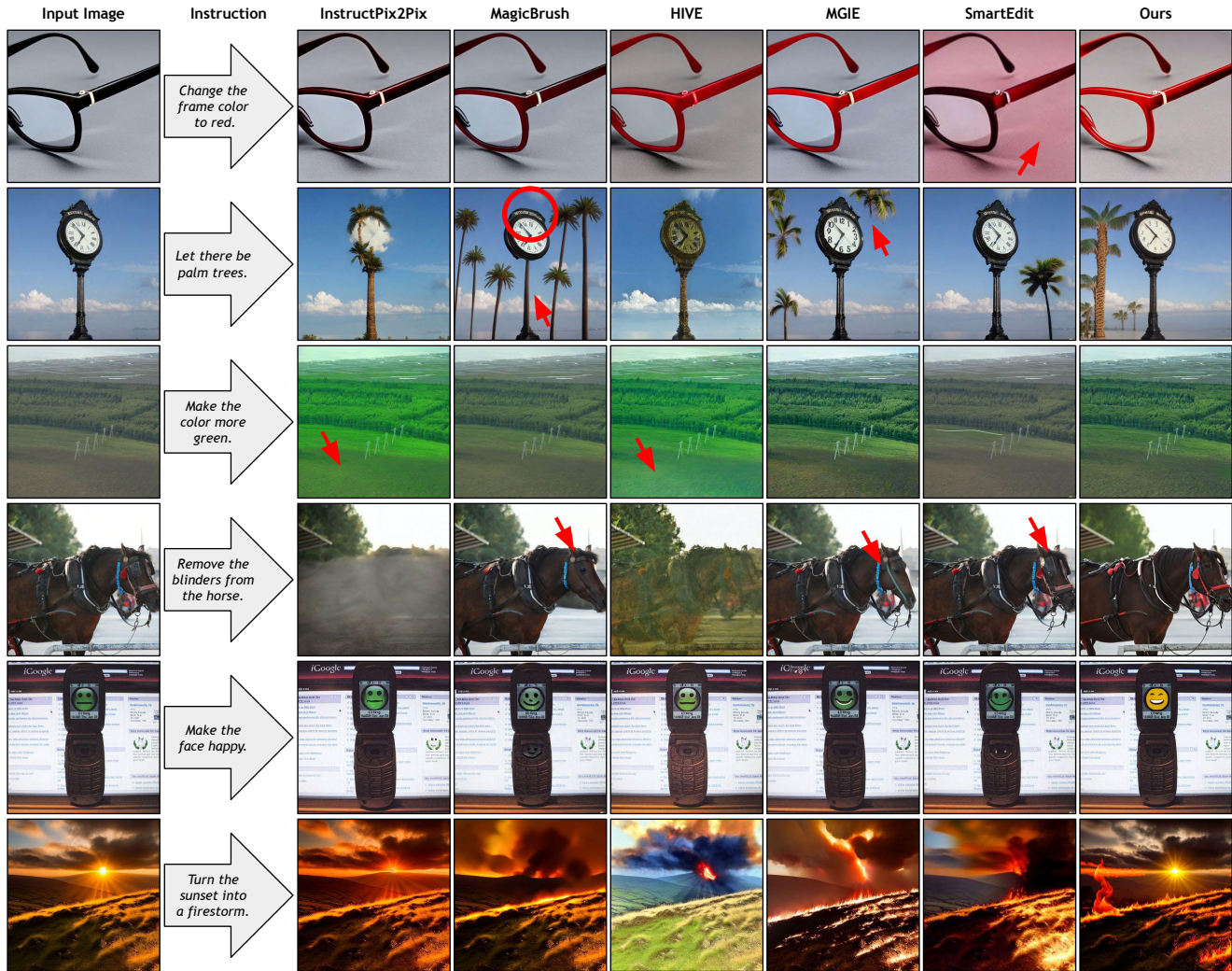


Figure 8. **Qualitative comparison of our method with baseline models for various editing instructions.** From left to right: Input image, edit instruction, and results from InstructPix2Pix, MagicBrush, HIVE, MGIE, SmartEdit, and our method. Our approach demonstrates superior fidelity and alignment with the provided instructions across diverse tasks, such as expression changes, color adjustments, object transformations, and creative edits. Red circles and arrows indicate drastic problems during the image editing.

moval, style changes, and complex scene edits.

The comparison highlights that our method consistently achieves higher fidelity and better alignment with the provided instructions. For instance, when instructed to modify facial expressions, such as “make the face happy,” our method produces more natural and expressive results. Similarly, for color adjustments, such as “make the color more green,” our approach ensures vibrant and accurate edits that surpass the performance of baseline models. In more challenging scenarios, like “turn the sunset into a firestorm,” our method maintains the structural integrity of the original image while executing the desired transformations. Furthermore, in creative edits, such as “remove the blinders from the horse,” our model demonstrates exceptional precision

and attention to detail.

F. Additional Quantitative Results

F.1. Evaluation on PIE-Bench

We apply our method to the PIE benchmark [22] to evaluate its performance on diverse editing tasks and compare it to IP2P, a representative feed-forward instruction-based editing method and a supervised alternative to our approach. Table 4 summarizes the results. The results show that our method outperforms IP2P across most metrics, including better preservation of structure (PSNR and SSIM), lower perceptual differences (LPIPS), and reduced mean squared error (MSE). These improvements demonstrate the scalabil-

ity and versatility of our approach on a broader benchmark. This analysis is included in the revised manuscript to provide a comprehensive evaluation of our method.

Table 4. **Performance comparison on the PIE benchmark.** Lower values for Distance, LPIPS, and MSE indicate better performance, while higher values for PSNR, SSIM, Whole, and Edit indicate improved quality and structural preservation.

Methods	Distance ↓	PSNR ↑	LPIPS ↓	MSE ↓	SSIM ↑	Whole ↑	Edit ↑
InstructDiffusion	75.44	20.28	155.66	349.66	75.53	23.26	21.34
IP2P	57.91	20.82	158.63	227.78	76.26	23.61	21.64
Ours	27.05	26.85	60.57	40.07	83.69	24.78	21.89

F.2. Evaluation on Emu Edit

We apply our method to the Emu Edit benchmark [43] to evaluate its performance on diverse editing tasks and compare it to other baselines. Table 5 presents a quantitative comparison across multiple metrics, assessing the quality of the generated edits. Our approach achieves the best results across most metrics, including higher CLIP scores, which indicate better alignment with textual descriptions, and improved perceptual quality as measured by DINO. Notably, our method surpasses all baselines in $CLIP_{dir}$ and $CLIP_{im}$, demonstrating stronger instruction adherence and output realism. The improvements in these objective measures further support the effectiveness of our method in complex editing tasks.

Table 5. **Performance comparison on the Emu Edit benchmark.** Comparison with image-editing baselines evaluated on Emu Edit test set. For each method, we report CLIP, L1, and DINO metrics.

Method	$CLIP_{dir}$ ↑	$CLIP_{im}$ ↑	$CLIP_{out}$ ↑	L1 ↓	DINO ↑
InstructPix2Pix [6]	0.078	0.834	0.219	0.121	0.762
MagicBrush [58]	0.090	0.838	0.222	0.100	0.776
PnP [50]	0.028	0.521	0.089	0.304	0.153
Null-Text Inv. [31]	0.101	0.761	0.236	0.075	0.678
Emu Edit [43]	0.109	0.859	0.231	0.094	0.819
Ours	0.115	0.867	0.244	0.083	0.834

F.3. Evaluation on MagicBrush Test

In this section, we present the full quantitative analysis on the MagicBrush test set, including results from both global description-guided and instruction-guided models, as shown in Tab. 6. While our method, UIP2P, is not fine-tuned on human-annotated datasets like MagicBrush, it still achieves highly competitive results compared to models specifically fine-tuned for the task. In particular, UIP2P demonstrates either the best or second-best performance in key metrics such as L1, L2, and CLIP-I, even outperforming fine-tuned models in several cases. This highlights the robustness and generalization capabilities of UIP2P, showing that it can effectively handle complex edits without the

need for specialized training on real datasets. These results further validate that UIP2P delivers high-quality edits in a variety of contexts, maintaining competitive performance against fine-tuned models on the MagicBrush dataset, which is human-annotated.

Table 6. **Quantitative comparison on MagicBrush [58] test set.** In the multi-turn setting, target images are iteratively edited from the initial source images. Best results are in **bold**.

Settings	Methods	L1 ↓	L2 ↓	CLIP-I ↑	DINO ↑	CLIP-T ↑
<i>Global Description-guided</i>						
	Open-Edit [27]	0.1430	0.0431	0.8381	0.7632	0.2610
	VQGAN-CLIP [10]	0.2200	0.0833	0.6751	0.4946	0.3879
	SD-SDEdit [30]	0.1014	0.0278	0.8526	0.7726	0.2777
	Text2LIVE [3]	0.0636	0.0169	0.9244	0.8807	0.2424
	Null Text Inversion [31]	0.0749	0.0197	0.8827	0.8206	0.2737
<i>Single-turn</i>						
<i>Instruction-guided</i>						
	HIVE [59]	0.1092	0.0341	0.8519	0.7500	0.2752
	w/ MagicBrush [58]	0.0658	0.0224	0.9189	0.8655	0.2812
	InstructPix2Pix [6]	0.1122	0.0371	0.8524	0.7428	0.2764
	w/ MagicBrush [58]	<u>0.0625</u>	0.0203	0.9332	<u>0.8987</u>	0.2781
	UIP2P w/ IP2P Dataset	0.0722	0.0193	0.9243	0.8876	0.2944
	UIP2P w/ CC3M Dataset	0.0680	0.0183	0.9262	0.8924	<u>0.2966</u>
	UIP2P w/ CC12M Dataset	0.0619	<u>0.0174</u>	<u>0.9318</u>	0.9039	0.2964
<i>Global Description-guided</i>						
	Open-Edit [27]	0.1655	0.0550	0.8038	0.6835	0.2527
	VQGAN-CLIP [10]	0.2471	0.1025	0.6606	0.4592	0.3845
	SD-SDEdit [30]	0.1616	0.0602	0.7933	0.6212	0.2694
	Text2LIVE [3]	0.0989	0.0284	0.8795	0.7926	0.2716
	Null Text Inversion [31]	0.1057	0.0335	0.8468	0.7529	0.2710
<i>Multi-turn</i>						
<i>Instruction-guided</i>						
	HIVE [59]	0.1521	0.0557	0.8004	0.6463	0.2673
	w/ MagicBrush [58]	<u>0.0966</u>	0.0365	0.8785	0.7891	0.2796
	InstructPix2Pix [6]	0.1584	0.0598	0.7924	0.6177	0.2726
	w/ MagicBrush [58]	0.0964	0.0353	0.8924	0.8273	0.2754
	UIP2P w/ IP2P Dataset	0.1104	0.0358	0.8779	0.8041	0.2892
	UIP2P w/ CC3M Dataset	0.1040	0.0337	0.8816	0.8130	<u>0.2909</u>
	UIP2P w/ CC12M Dataset	0.0976	<u>0.0323</u>	<u>0.8857</u>	<u>0.8235</u>	0.2901

G. Edit Reversibility Constraint Example

We demonstrate ERC with a visual example during inference. In the forward pass, the model transforms the input image based on the instruction (e.g., “turn the forest path into a beach”). In the reverse pass, the corresponding reverse instruction (e.g., “turn the beach back into a forest”) is applied, reconstructing the original image. This showcases the model’s ability to maintain consistency and accuracy across complex edits, ensuring that both the forward and reverse transformations align coherently. Additional examples, such as adding and removing objects, further emphasize UIP2P’s adaptability in diverse editing tasks. Figure 9 illustrates how our method ensures precise, reversible edits while maintaining the integrity of the original content.

H. Dataset Details

H.1. LLM Prompts for Data Generation

To ensure reproducibility, we provide the exact prompts used with LLMs for generating reverse instructions and expanding datasets. These prompts were crucial for creating

Table 7. **Examples of Four Possible Edits for Two Different Input Captions.** Our dataset generation process showcases the flexibility of the reverse instruction dataset by demonstrating multiple transformations for the same caption.

Input Caption	Edit Instruction	Edited Caption	Reverse Instruction
A dog sitting on a couch	change the dog's color to brown	A brown dog sitting on a couch	change the dog's color back to white
	add a ball next to the dog	A dog sitting on a couch with a ball	remove the ball
	remove the dog	An empty couch	add the dog back
	move the dog to the floor	A dog sitting on the floor	move the dog back to the couch
A car parked on the street	change the car color to red	A red car parked on the street	change the car color back to black
	add a bicycle next to the car	A car parked on the street with a bicycle	remove the bicycle
	remove the car	An empty street	add the car back
	move the car to the garage	A car parked in the garage	move the car back to the street

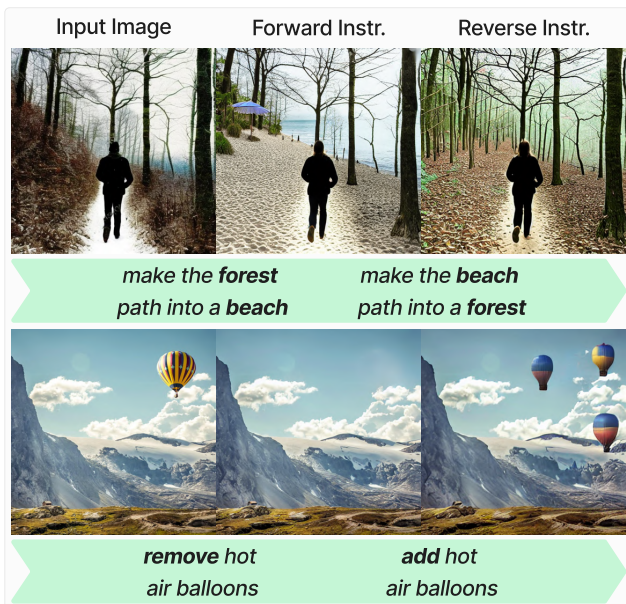


Figure 9. Forward and reverse edits are applied sequentially.

the training data without requiring ground-truth edited images.

H.1.1. LLM Prompt for Reverse Instruction Generation (IP2P Dataset)

Below is an instruction that describes a task, paired with an input that provides further context. Write a response that appropriately completes the request.

Instruction:

You are an expert in image editing instructions. Given an input caption, an edit instruction, and the resulting edited caption, generate a reverse instruction that would undo the edit and return to the original state.

Input:

Input Caption: "{input_caption}"
 Edit Instruction: "{edit_instruction}"
 Edited Caption: "{edited_caption}"

Examples:

- Input: "A man wearing a denim jacket"
 -> "make the jacket a rain coat"
 -> "A man wearing a rain coat"
 Reverse: "make the coat a denim jacket"
- Input: "A sofa in the living room"
 -> "add pillows" -> "A sofa in the living room with pillows"
 Reverse: "remove the pillows"

Response:

{reverse_instruction}

H.1.2. LLM Prompt for Multi-Edit Generation (CC3M/CC12M)

Below is an instruction that describes a task, paired with an input that provides further context. Write a response that appropriately completes the request.

Instruction:

Given an input caption, generate 4

different edit instructions along with their corresponding edited captions and reverse instructions. Focus on diverse edit types: color changes, object addition/removal, and positional changes. Ensure edits are realistic and reversible.

```
### Input:
Input Caption: "{input_caption}"

### Response:
1. Edit Instruction: [instruction]
   Edited Caption: [result]
   Reverse Instruction: [undo instruction]

2. Edit Instruction: [instruction]
   Edited Caption: [result]
   Reverse Instruction: [undo instruction]

3. Edit Instruction: [instruction]
   Edited Caption: [result]
   Reverse Instruction: [undo instruction]

4. Edit Instruction: [instruction]
   Edited Caption: [result]
   Reverse Instruction: [undo instruction]
```

H.2. Dataset Filtering

We apply CLIP [36] to both the CC3M [42] and CC12M [8] datasets to calculate the similarity between captions and images, ensuring that the text descriptions accurately reflect the content of the corresponding images. Following the methodology used in InstructPix2Pix (IP2P) [6], we adopt a CLIP-based filtering strategy with a similarity threshold set at 0.2. This threshold filters out image-caption pairs that do not have sufficient semantic alignment, allowing us to curate a dataset with higher-quality text-image pairs. For the filtering process, we utilize the CLIP ViT-L/14 model, which provides a robust and well-established framework for capturing semantic similarity across text and images.

By applying this filtering process, we ensure that only relevant and coherent pairs remain in the dataset, improving the quality of training data and helping the model better generalize to real-world editing tasks. As a result, the filtered CC3M dataset contains 2.5 million image-caption pairs, while the filtered CC12M dataset contains 8.5 million pairs. This careful curation of the dataset enhances the reliability of the training process without relying on human annotations, making it scalable for broader real-image datasets without the cost and limitations of human-annotated ground-truth datasets [6, 58].

H.3. More Examples from Reverse Instructions Dataset

To demonstrate the versatility of our reverse instruction dataset, we provide examples with multiple variations of edits for two different input captions. Each caption has four distinct edits, such as color changes, object additions, object removals, and positional adjustments. This variety helps the model generalize across a wide range of tasks and scenarios, as discussed in Sec. 4.2, main paper. The use of large language models (LLMs) to generate reverse instructions further enhances the flexibility of our dataset.

These examples, along with others in Tab. 1, illustrate the diversity of edit types our model learns, enabling it to perform a wide range of tasks across different real-image datasets. The reverse instruction mechanism ensures that the edits are reversible, maintaining consistency and coherence in both the forward and reverse transformations.

I. Additional Implementation Details

I.1. Details of Competitor Methods

Our method offers significant advantages over competitors in both training and inference. Unlike supervised methods that rely on paired triplets of input images, edited images, and instructions, our approach eliminates the need for such datasets, reducing biases and improving scalability. For example, MagicBrush is fine-tuned on a human-annotated dataset, while HIVE leverages Prompt-to-Prompt editing with human annotators, introducing dependency on labor-intensive processes. Furthermore, MGIE and SmartEdit rely on LLMs during inference, which significantly increases computational overhead. These distinctions highlight the efficiency and practicality of our approach, as it avoids the need for expensive human annotations and additional inference-time complexities. Like other editing methods, our approach can produce small variations for different random seeds but consistently applies the specified edit, eliminating the need for manual selection. To the best of our knowledge, the compared methods, *e.g.*, MagicBrush, InstructPix2Pix or other methods, also do not involve manual selection.

InstructPix2Pix [6] is a diffusion-based model that performs instruction-based image editing by training on triplets of input image, instruction, and edited image¹. The model is fine-tuned on a synthetic dataset of edited images generated by combining large language models (LLMs) and Prompt-to-Prompt [17]. This approach relies on paired datasets, which can introduce biases and limit generalization. InstructPix2Pix serves as one of the key baselines for our comparison, given its supervised training methodology.

¹<https://github.com/timothybrooks/instruct-pix2pix>

HIVE [59] is an instruction-based editing model that fine-tunes InstructPix2Pix based on human feedback². Specifically, HIVE learns from user preferences about which edited images are preferred, incorporating this feedback into the model training. While this approach allows HIVE to better align with human expectations, it still builds on top of InstructPix2Pix and does not start training from scratch. This limits its flexibility compared to methods like UIP2P, which are trained from the ground up.

MagicBrush [58] fine-tunes the pre-trained weights of InstructPix2Pix on a human-annotated dataset to improve real-image editing performance³. While this fine-tuning approach makes MagicBrush highly effective for specific tasks with ground-truth labels, it limits its generalizability compared to methods like UIP2P, which are trained from scratch. Moreover, MagicBrush’s reliance on human-annotated data introduces significant scalability challenges, as obtaining such annotations is both costly and labor-intensive. This dependency makes it less suited for broader datasets where large-scale annotations may not be feasible.

MGIE [12] introduces a large multimodal language model to generate more precise instructions for image editing⁴. Like InstructPix2Pix, MGIE requires a paired dataset for training but uses the language model to improve the quality of the instructions during inference. However, this reliance on LLMs during inference adds computational overhead. In contrast, UIP2P operates without LLMs at inference time, reducing overhead while maintaining flexibility.

SmartEdit [20] is based on InstructDiffusion, a model already trained for instruction-based image editing tasks⁵. It introduces a bidirectional interaction module to improve text-image alignment, but its reliance on the pre-trained InstructDiffusion limits flexibility, as SmartEdit does not start training from scratch. Additionally, SmartEdit depends on large language models (LLMs) during inference, increasing computational overhead. This makes SmartEdit less efficient than UIP2P in scenarios where real-time or large-scale processing is required.

DiffusionCLIP [25] leverages pre-trained diffusion models for text-driven image manipulation by fine-tuning the reverse diffusion process with a CLIP-based loss⁶. Unlike UIP2P, which enforces edit reversibility constraints for unsupervised training, DiffusionCLIP relies on fine-tuning for each new target attribute, making it less scalable for large-scale instruction-based editing. Additionally, its approach requires per-attribute model tuning and inversion of the input image before the editing process, leading to increased training and inference overhead compared to UIP2P, which

generalizes across a diverse set of edits without explicit supervision and additional inversion process.

During evaluation, we use the publicly available implementations and demo pages of the baseline methods. Each baseline provides a different approach to instruction-based image editing, and together they offer a comprehensive set of methods for comparing the performance, flexibility, and efficiency of the proposed method, UIP2P.

I.2. Code Implementation Overview

Our UIP2P implementation with ERC builds on existing frameworks for reproducibility:

- **Base Framework:** The code is based on Instruct-Pix2Pix⁷, which provides the foundation for instruction-based image editing.
- **Adopted CLIP Losses:** We adopted and modified CLIP-based loss functions from StyleGAN-NADA⁸ to fit ERC, improving image-text alignment for our specific tasks.

I.3. Algorithm Overview

In this section, we explain the proposed method, UIP2P, which introduces unsupervised learning for instruction-based image editing. The core of our approach is the Edit Reversibility Constraint (ERC), which ensures that edits are coherent and reversible when applied sequentially in both forward and reverse instructions.

The algorithm consists of two key processes:

- **Forward Process:** Starting with an input image and a forward edit instruction, noise is first added to the image. The model then predicts the noise, which is applied to reverse the noise process and recover the edited image (*see Algorithm 1, lines 2-4*).
- **Reverse Process:** Given the forward-edited image and a reverse edit instruction, noise is applied again. The model predicts the reverse noise, which is used to undo the edits and reconstruct the original image. This ensures that the reverse edits are consistent with the original input image (*see Algorithm 1, lines 6-8*).

ERC is applied between the original input image, the forward-edited image, and the reconstructed image, along with their respective attention maps and captions (*see Algorithm 1, line 10*). The \mathcal{L}_{ERC} function guides the model’s learning through backpropagation (*see Algorithm 1, lines 12-13*).

J. Limitations and Failure Cases

While our method demonstrates strong performance across various editing tasks, we acknowledge several limitations. Our reliance on CLIP for semantic alignment in-

²<https://github.com/salesforce/HIVE>

³<https://github.com/OSU-NLP-Group/MagicBrush>

⁴<https://ml-mgie.com/playground.html>

⁵<https://github.com/TencentARC/SmartEdit>

⁶<https://github.com/gwang-kim/DiffusionCLIP.git>

⁷<https://github.com/timothybrooks/instruct-pix2pix>

⁸<https://github.com/rinongal/StyleGAN-nada>

Algorithm 1 Unsupervised Instruction-Based Image Editing (UIP2P) with ERC

works beyond CLIP-based metrics.

Require: Image I_i (input image), Forward edit instruction F , Reverse edit instruction R , Noise levels t (forward), \hat{t} (reverse), Model M , Loss function L_{ERC} , Noise function N , Input caption T_i , Edited caption T_e

Ensure: Edited image I_e , Reconstructed image I_r

1: **Forward Process:**

- 2: $z_t \leftarrow N(I_i, t)$ \triangleright Add noise t to the input image I_i
- 3: $\hat{\epsilon}_F, A_f \leftarrow M(z_t|I_i, F)$ \triangleright Model M predicts forward noise $\hat{\epsilon}_F$ and extracts attention map A_f
- 4: $I_e \leftarrow \text{Apply}(\hat{\epsilon}_F, z_t, t)$ \triangleright Apply predicted noise $\hat{\epsilon}_F$ to reverse the process of obtaining z_t and recover I_e

5: **Reverse Process:**

- 6: $z_{\hat{t}} \leftarrow N(I_e, \hat{t})$ \triangleright Add noise \hat{t} to the forward-edited image I_e
- 7: $\hat{\epsilon}_R, A_r \leftarrow M(z_{\hat{t}}|I_e, R)$ \triangleright Model M predicts reverse noise $\hat{\epsilon}_R$ and extracts attention map A_r
- 8: $I_r \leftarrow \text{Apply}(\hat{\epsilon}_R, z_{\hat{t}}, \hat{t})$ \triangleright Apply predicted noise $\hat{\epsilon}_R$ to reverse the process of obtaining $z_{\hat{t}}$ and recover I_r

9: **Edit Reversibility Constraint Loss:**

- 10: $L_{ERC} \leftarrow L(I_i, I_e, I_r, A_f, A_r, T_i, T_e)$ \triangleright Compute ERC loss using I_i, I_e, I_r , attention maps A_f, A_r , input text T_i , and edited text T_e

11: **Update Model:**

- 12: Backpropagate the loss L_{ERC} and update the model M
 - 13: Repeat until convergence
-

troduces challenges in fine-grained spatial reasoning, object counting, and complex compositional understanding. The method may struggle with instructions requiring precise spatial relationships (*e.g.*, “add three apples to the left of the table”) or complex multi-object scenarios with occlusions. Additionally, like many diffusion-based methods, our approach has difficulties with text rendering, extreme lighting changes, and cases requiring simultaneous style transfer with significant structural modifications.

Our method’s performance is also constrained by training data quality and the reverse instruction generation process using LLMs. While more efficient than LLM-based approaches during inference, the training process requires additional computational overhead for generating reverse instructions and computing attention consistency losses. Future work could address these limitations by integrating stronger multimodal models for better spatial understanding, incorporating perceptual losses for improved photorealism, and developing more sophisticated evaluation frame-